Macromolecules **2006,** *39,* 5015−5020

Exploring the Limits of Branching and Gel Content in the Emulsion Polymerization of *n*-BA

Iñigo González, José R. Leiza, and José M. Asua*

Institute for Polymer Materials, POLYMAT and Grupo de Ingeniería Química, Dpto. de Química Aplicada, Facultad de Ciencias Químicas, The University of the Basque Country, P.O Box 1072, 20080 Donostia-San Sebastián, Spain

Received March 17, 2006; Revised Manuscript Received May 16, 2006

ABSTRACT: The possibility of synthesizing a highly branched poly(*n*-butyl acrylate) by emulsion polymerization was explored. Branching levels as high as 6.3% were obtained at high temperatures under starved conditions. Gel, which ranged from 53% to 78%, increased with temperature and process time. Highly branched polymers with gel contents of about 70% showed a very good shear resistance. It was found that the polymerization rate decreased with temperature. The mechanisms responsible for this surprising kinetics as well as for the formation of the microstructure were discussed.

Introduction

Because of the commercial importance of the *n*-butyl acrylate-based emulsion polymers and its intriguing polymerization mechanisms, the emulsion polymerization of *n*-BA has been extensively investigated.[1−12] During polymerization tertiary radicals are produced by both intermolecular and intramolecular (backbiting) transfer to polymer.[13,14] These tertiary radicals are less reactive than the secondary ones and lower the polymerization rate.[1,2,15] Propagation of the tertiary radicals yields branched polymers. Intermolecular chain transfer to polymer yields long chain branches (LCB). When intermolecular chain transfer to polymer is followed by termination by combination, gel is formed. On the other hand, intramolecular transfer to polymer produces short chain branches (SCB). Plessis et al.[1,2] showed that gel and total branches were not correlated and that in the polymerization of *n*-butyl acrylate most branches are generated by backbiting. Therefore, the branching frequency can be calculated as the ratio between the rate of backbiting and the overall rate of polymerization:

$$\text{branching level} = \frac{\text{rate of branch formation}}{\text{rate of polymerization}} \approx \frac{k_{bb}P_1}{(k_{p1}P_1 + k_{p2}P_2)[\mathrm{M}]_p} \quad (1)$$

where k_{bb} is the intramolecular transfer to polymer rate constant, k_{p1} and k_{p2} are the propagation rate constants for secondary and tertiary radicals, respectively, $[\mathrm{M}]_p$ is the monomer concentration in the particles, and P_1 and P_2 are the probabilities of having a secondary radical (R_1) or tertiary radical (R_2) as the terminal unit in the growing chain:[2]

$$P_1 = \frac{R_1}{R_1 + R_2} = \frac{k_{p2}[\mathrm{M}]_p}{k_{p2}[\mathrm{M}]_p + k_{bb}}; \quad P_2 = 1 - P_1 \quad (2)$$

Combination of eqs 1 and 2 yields

$$\text{branching level} \approx \frac{k_{bb}}{k_{p1}[\mathrm{M}]_p + k_{bb}} \quad (3)$$

Equation 3 shows that the branching frequency is inversely proportional to the concentration of monomer in the polymer particles. This agrees with the level of branching measured by Plessis et al.[2,6] using ^{13}C NMR spectroscopy in a series of seeded semibatch emulsion polymerizations of *n*-BA carried out at 75 °C. Equation 3 predicts a high level of branching at very low monomer concentrations. This will result in a different polymer architecture which may have interesting properties. Therefore, in this work the possibility of synthesizing a highly branched poly(*n*-butyl acrylate) is explored.

To synthesize this polymer, semibatch emulsion polymerizations of *n*-BA were carried out under extremely starved conditions, i.e., using very low monomer concentrations in the polymer particles. This was achieved by using long process times. In addition, formation of branches was enhanced by working at high temperatures because of the higher activation energy of the intramolecular transfer to polymer (29 kJ/mol)[17] as compared to that of the propagation reaction (17.9 kJ/mol).[18] It is worth pointing out that the maximum temperature is limited by the occurrence of β-scission.[19,20] Nevertheless, the effect of β-scission is not significant at temperatures below 110 °C.

The article is organized as follows: First, the experimental procedure and characterization techniques employed are presented. Then, the results obtained are presented and discussed in terms of polymerization kinetics and microstructure of the polymers produced. Finally, the effect of branching on the adhesive properties (tack and shear resistance) of the latexes produced was analyzed.

Experimental Section

Materials. *n*-Butyl acrylate (*n*-BA, Quimidroga) and acrylic acid (AA, Aldrich) were used as received. Sodium lauryl sulfate (Aldrich) was used as emulsifier on the seed preparation and ABEX2005 (Rhodia) in the semicontinuous experiments. Sodium bicarbonate (PANREAC) was used as buffer in the preparation of the seed. Potassium persulfate (Fluka Chemika) was used as initiator.

Emulsion Polymerizations. All the semicontinuous reactions were seeded. The poly(*n*-BA) seed used in the semicontinuous

---

* To whom correspondence should be addressed: e-mail jm.asua@ehu.es; Tel (+34) 943018184; Fax (+34) 943015270.

10.1021/ma060603g CCC: $33.50

Table 1. Formulation Used To Prepare the Seed

	amount (g)
n-butyl acrylate	250
water	1000
SLS	5.00
$NaHCO_3$	1.25
$K_2S_2O_8$	1.25
seed properties	
solids content	20.1
gel content	<1%
particle size[a]	67 nm

[a] Intensity average measured by DLS.

Table 2. Formulation Used in the Seeded Semicontinuous Emulsion Polymerization of *n*-BA (Feeding Times: 3 and 12 h)

	initial charge (g)	stream 1 (g)	stream 2 (g)
seed polymer	20		
water[a]	97.5	29	235
ABEX2005	1.25		2.5
n-butyl acrylate			225.4
acrylic acid			4.6
$K_2S_2O_8$	0.338	0.338	

[a] Includes the water contained in the seed.

Table 3. Formulation Used in the Seeded Semicontinuous Emulsion Polymerization of *n*-BA (Feeding Time: 24 h)

	initial charge (g)	stream 1 (g)	stream 2 (g)	stream 3 (g)
seed polymer	26			
water[a]	137.78		155.75	184.07
ABEX2005	1.625		3.25	
n-butyl acrylate		293.02		
acrylic acid		5.98		
$K_2S_2O_8$	0.401			0.478

[a] Includes the water contained in the seed.

experiments was prepared batchwise following the formulation shown in Table 1 in a stainless steel reactor fitted with a sampling device, N_2 inlet, and a stainless steel impeller. Table 1 also includes the properties of the seed. The reaction was carried out at 65 °C, and it was kept overnight at 90 °C with the aim of decomposing the unreacted initiator.

The semicontinuous emulsion polymerizations were carried out in a 1 L glass jacketed reactor fitted with a reflux condenser, sampling device, N_2 inlet, two feeding inlets and a stainless steel anchor stirrer equipped with two blade impellers rotating at 230 rpm. Table 2 summarizes the formulation used in the semicontinuous experiments.

Because of the difficulties in maintaining the preemulsion stable for long periods of time, in the 24 h experiments, neat monomer addition was used (Table 3).

The experimental procedure was as follows: First, the polymer seed (dp = 67 nm and 20.1% solids content) and a part of the emulsifier were added into the reactor. When the temperature was 0.5 °C below the reaction temperature set point, half of the initiator was added to the reactor. When the desired reactor temperature was reached, the rest of the ingredients were fed over the process time. Upon finishing the addition, the reaction was kept batchwise for 60 min.

Characterization. Samples were extracted from the reactor, and the reaction was short-stopped with hydroquinone. Unreacted monomer was measured by headspace chromatography, using a Hewlett-Packard HP7694E headspace sampler and a Hewlett-Packard HP6890GC chromatograph with a FID detector. 4-Methyl-2-pentanone was used as internal standard. The instantaneous conversion was defined as the amount of polymer divided by the amount of monomer and polymer in the reactor. The overall conversion was the amount of polymer divided by the total amount of monomer plus polymer in the formulation.

Particle size was measured by dynamic light scattering (Coulter N4-Plus). The analysis was carried out at 25 °C with the detector at an angle of 90°. Each sample was analyzed three times with a previous 6 min equilibration time, and only samples containing baseline errors below 1% were considered to calculate the average. The results obtained by this technique were used to calculate the total number of polymer particles.

The gel fraction was determined by extraction with THF. The process consisted in a 7 h continuous extraction with THF under reflux in a 2 L glass reactor. 2 h of extraction was enough to extract 90% of the total sol fraction. After the extraction, the samples were dried, and the gel content was calculated as the ratio between the dry polymer remaining after the extraction and the initial amount of dry polymer. It is worth pointing out that the gel measured by this method contained both cross-linked polymer and entangled high molecular weight polymer chains.

Swelling experiments were carried out in methyl ethyl ketone (MEK) at room temperature for 24 h. The latex used in this experiment was coagulated using a $CaCl_2$ solution, and the coagulum was dried in an oven at 60 °C for 3 days. The swelling value (which is inversely proportional to the cross-linking density) was calculated as the ratio between the weight of the swollen gel polymer and the dry weight of the gel polymer.

The sol molecular weight was determined by size exclusion chromatography (SEC,Waters). The setting consists of a pump (Waters 510), a Viscotek 250 dual detector formed by a differential refractometer and a viscosimeter and three columns in series (Styragel HR2, HR4, and HR6; with a pore size from 10^2 to 10^6 Å). The analysis were performed at 35 °C, and THF was used as solvent at a flow rate of 1 mL/min. A droplet of latex was directly added to THF, the soluble part was filtered (polyamide filter diameter = 0.45 μm), and the sample was injected in the equipment.

The level of branching was measured by liquid ^{13}C NMR using a Bruker Avance DPX 300 spectrometer with a BBO probe operating at 75.5 MHz. Latex samples were dried and swollen in $CDCl_3$ before the analysis. Samples were analyzed with NOE effect suppression by inverse gate decoupling with a pulse interval of 4 s. Over 25 000 acquisitions were collected in acquisition times longer than 24 h to have a good signal/noise ratio. The peak assignment were made according to Lovell et al.,[7] and the level of branching was calculated as in ref 2.

The adhesive properties of the latex films were assessed by determining the resistance to shear and tack. Shear resistance is the property of an adhesive to remain adhered under load applied parallel to the surface of the tape. It was assessed by the holding power shear test.[21] This test consists on applying a standard area of tape (25 × 25 mm) on a panel 2° to the vertical holding a 1 kg load until failure. The time elapsed between application of the load and the complete separation is the measurement of the resistance to shear. Tack is the property related to the capacity of an adhesive to form bonds with a surface after brief contact under light pressure. It was assessed by using the rolling ball tack test.[22] This test consists of releasing a stainless steel ball (11 mm diameter) at the top of an inclined track, to come into contact at the bottom of the track with a horizontal upward-facing adhesive. The roll-out distance that the ball travels over the film is an inverse scale of tack; i.e., the longer the distance the ball travels across the adhesive before stopping, the lower the tack.

Results and Discussion

Polymerization Kinetics. Figure 1 shows the evolution of the instantaneous conversion for different feeding times and temperatures. It can be seen that in the polymerizations carried out with feeding times of 3 and 12 h the instantaneous conversion at 95 °C was lower than those carried out at 75 and 85 °C. In addition, in the runs carried out with 24 h of feeding time, the instantaneous conversion decreased as temperature increased. This was surprising as an increase of the polymerization rate with temperature was expected. It is worth pointing out that the conversion was determined by measuring the

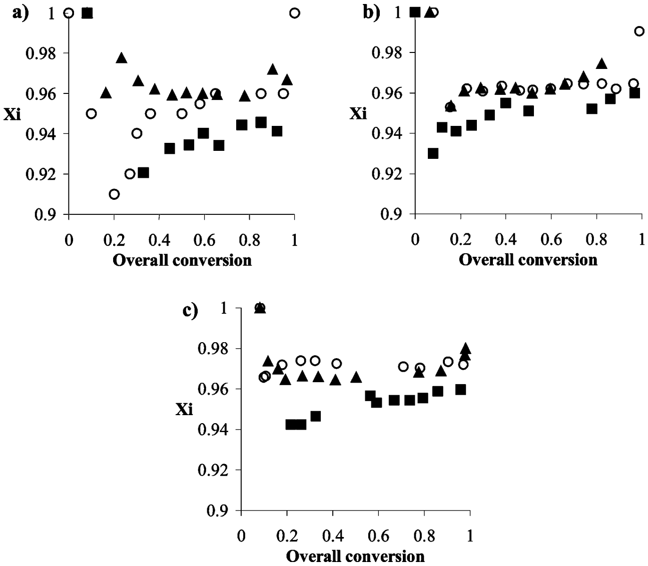

Figure 1. Effect of the reaction temperature on the evolution of the instantaneous conversion in the seeded semibatch emulsion polymerization of *n*-BA carried out at different feeding times: (a) 3 h, (b) 12 h, (c) 24 h. Legend: (○) 75 °C, (▲) 85 °C, (■) 95 °C.

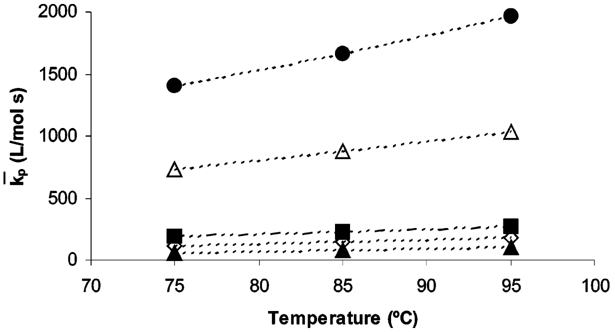

Figure 2. Simulated $\bar{k}_p$ values calculated from eq 1 for the emulsion polymerization of *n*-BA at different temperatures and monomer concentrations in the particle. Legend: (▲) 0.01 mol/L, (◇) 0.05 mol/L, (■) 0.1 mol/L, (△) 0.5 mol/L; (●) 1 mol/L. Frequency factors: $k_{p10} = 2.21 \times 10^7$ L/(mol s);[18]; $k_{p20} = 1.25 \times 10^6$ L/(mol s);[23] $k_{bb0} = 4.31 \times 10^7$ L/(mol s).[23] Activation energies: $E_{a,p1} = 17.9$ kJ mol^{-1};[18] $E_{a,p2} = 29.5$ kJ mol^{-1};[23] $E_{a,bb} = 29.8$ kJ mol^{-1}.[23]

unreacted monomer by headspace gas chromatography, which is a very accurate method in the range of conversions of Figure 1. Therefore, these results cannot be attributed to errors in the analytical method.

The polymerization rate (R_p) is given by

$$R_p = \bar{k}_p[M]_p\frac{\bar{n}}{N_A}N_p \tag{4}$$

where $\bar{k}_p$ is the apparent propagation rate constant, $[M]_p$ is the monomer concentration in the polymer particles, $\bar{n}$ is the average number of radicals per particle, N_A is the Avogadro's number, and N_p is the number of polymer particles per unit volume of water. The apparent propagation rate constant is given by

$$\overline{k_p} = k_{p1}P_1 + k_{p2}P_2 \tag{5}$$

According eq 4, temperature might influence the polymerization rate threefold: (i) through the apparent propagation rate constant, (ii) through the total number of polymer particles, and (iii) via the average number of radicals per particle.

Figure 2 plots the $\bar{k}_p$ values calculated from eqs 2 and 5 at different temperatures in a range of monomer concentrations in the particle spanning from 0.01 to 1 mol/L. It can be seen that the apparent propagation rate constant is a function of both temperature and monomer concentration. The effect of the concentration of monomer in the polymer particles on $\bar{k}_p$ is due to the fact that the probability of having tertiary radicals increases as the monomer concentration decreases.

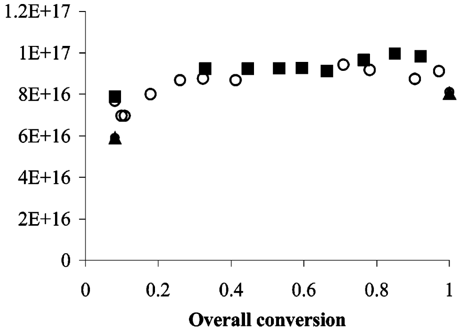

Figure 3. Evolution of the total number of polymer particles in the semicontinuous emulsion polymerization of *n*-BA produced at 24 h of feeding time. Legend: (○) 75 °C, (▲) 85 °C, (■) 95 °C.

Figure 2 shows that at lower monomer concentrations $\bar{k}_p$ was almost independent of temperature in the range from 75 to 95 °C. In this study, the polymerizations were carried out under rather starved conditions ($[M]_p \le 0.5$ M), and hence a modest effect of temperature on $\bar{k}_p$ was expected. However, this did not justify the decrease in the instantaneous conversion when temperature increased (Figure 1).

Figure 3 shows that the total number of polymer particles was roughly independent of the polymerization temperature at a feeding time of 24 h, and consequently they were not the cause of the decrease of the polymerization rate with temperature.

Calculation of the values of $\bar{n}$ from the values of the polymerization rate (obtained from Figure 1) and the number of particles using the apparent propagation rate coefficients showed that the average number of radicals per particle was responsible for the decrease of the instantaneous conversion when increasing the reaction temperature. Attempts to elucidate the reasons of these results by means of theoretical calculations were carried out. However, the theoretical estimation of $\bar{n}$ was uncertain because the values of the entry and exit rate coefficients were not available. Therefore, it was decided to estimate the effect of temperature on the radical concentration in a homogeneous system. It should be pointed out that radical compartmentalization will determine the total radical concentration in a dispersed system. Nevertheless, as the number of particles was roughly the same in all cases, it was assumed that the ratio between the concentration of radicals in the homogeneous system and that in the compartmentalized system was the same for all temperatures. Therefore, comparison between the radical concentrations calculated for homogeneous systems would serve as reference for the values of $\bar{n}$ in the compartmentalized system.

The radical concentration [R] is given by

$$[R] = \left(\frac{2f\,k_d[I]}{2k_t}\right)^{1/2} \tag{6}$$

where f ($f = 0.6$)[16] is the initiator efficiency factor, k_d ($k_d = 8 \times 10^{15}\exp(-1624/T)$[24]) is the initiator decomposition rate constant, [I] is the concentration of initiator in the reactor, and k_t ($k_t = 2.57\times 10^8 \exp(-292/T)$[25]) is the termination rate coefficient. It is worth pointing out that because of the presence

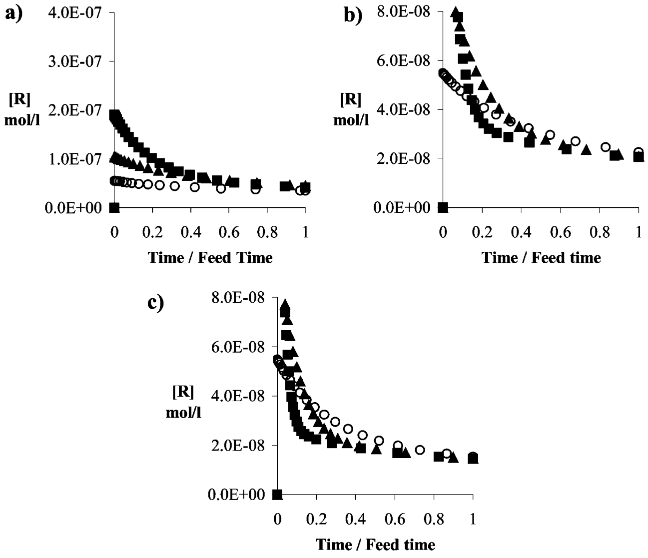

Figure 4. Simulated effect of the temperature on the evolution of the overall radical concentration at different feeding times: (a) 3 h, (b) 12 h, (c) 24 h. Legend: (○) 75 °C, (▲) 85 °C, (■) 95 °C.

of tertiary radicals, the effective k_t would be lower. Nevertheless, the effect would be similar in all cases not affecting the comparison.

The mass balance for the initiator is

$$\frac{\mathrm{d}[\mathrm{I}]}{\mathrm{d}t} = \frac{F_\mathrm{I}}{V} - k_\mathrm{d}[\mathrm{I}] \qquad (7)$$

where F_I is the initiator ($K_2S_2O_8$) feeding rate and V the volume of the reactor.

To reproduce the experimental procedure used in the semibatch emulsion polymerization experiments, the simulations were performed with the reactor initially filled with water and with half of the total amount of the initiator. The rest of the initiator was added at a constant flow rate for the corresponding feeding time. Only the initiator decomposition and the termination were accounted for, the termination rate coefficient being that corresponding to *n*-BA radicals.

Figure 4 presents the simulated overall concentration of radicals in a semibatch homogeneous polymerization process calculated at different temperatures and feeding times (3, 12, and 24 h). Figure 4 shows that at low feeding rates the higher the temperature the lower the radical concentration because the high decomposition rate of the initiator combined with the low feeding rate led to the depletion of the initiator. At high feeding rates, the effect was less acute but still apparent. These results, if extrapolated to the seeded semibatch emulsion polymerization of *n*-BA, indicate that the decrease of the instantaneous conversion with temperature was due to the depletion of initiator combined with the insensitivity of $\bar{k}_p$ to temperature variation at low $[M]_p$.

Polymer Microstructure. Figure 5 presents the level of branching as estimated from ^{13}C NMR measurements. It can be seen that branching increased with the feeding time and in less extent with temperature. The data obtained at 75 °C are plotted in Figure 6 together with the values obtained by Plessis et al.[2,6] and the predictions of eq 3.

It can be seen that with the parameters found in the literature (dotted lines) eq 3 overestimated the level of branches. The value used for k_{p1} complies with IUPAC recommended consistency checks and has been critically evaluated.[18] The value of k_{bb} is more uncertain as it was obtained from global fitting of kinetic data.[2] Actually, Peck et al.[20] reported a value for k_{bb} of 3000 s^{-1} at 138 °C which, using the same activation energy as that reported by Plessis et al.,[17] yielded a value of 644 s^{-1} at 75 °C. Even with this value (continuous line) eq 3 predicted a level of branches, at low $[M]_p$, significantly higher than that found experimentally. Further reduction of k_{bb} allows fitting the branching level at low $[M]_p$, but then the level of branches at higher monomer concentrations was underestimated (Figure 1). This suggests that eq 3 might not apply for the whole range of $[M]_p$ or that the value of k_{bb} decreased for low monomer concentrations, perhaps due to difficulties in the formation of the six-member ring (necessary for the backbitting mechanism) produced by the decrease of the free volume as the monomer concentration in the particles decreased.

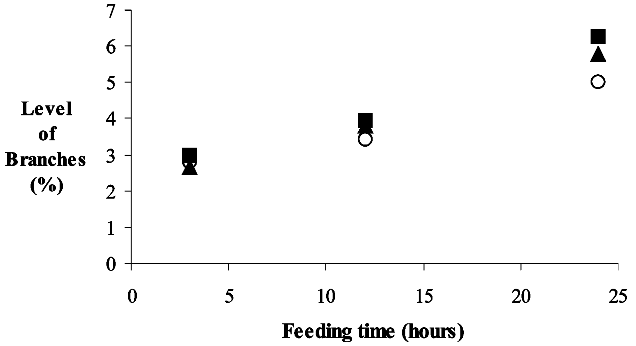

Figure 5. Final level of branching of poly(*n*-BA) latexes produced at different feeding times and temperatures. Legend: (○) 75 °C, (▲) 85 °C, (■) 95 °C.

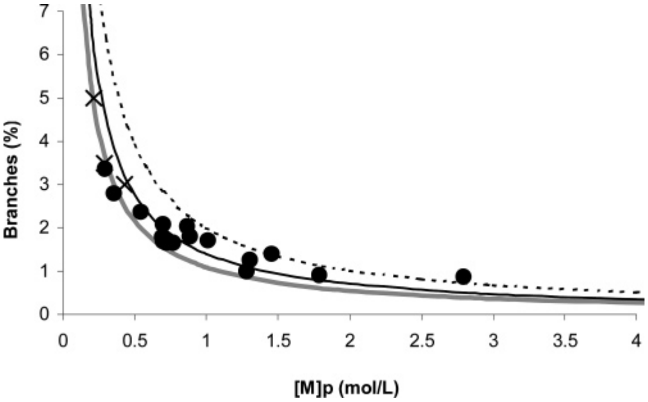

Figure 6. Effect of the monomer concentration on the branching level produced in the semibatch emulsion polymerization of *n*-BA at 75 °C. (●) Data from refs 2 and 6. (×) Data obtained in this work. (dashed line) Predictions of eq 3 with k_{p1} = 45 316 L/(mol s)[18] and k_{bb} = 924 s^{-1}.[2] (black line) Predictions of eq 3 with k_{p1} = 45 316 L/(mol s)[18] and k_{bb} = 644 s^{-1}.[20] (gray line) Predictions of eq 3 with k_{p1} = 45 316 L/(mol s)[18] and k_{bb} = 500 s^{-1}.

Figure 7 shows the gel content of the final latexes produced at different temperatures and monomer feeding times. For a given temperature, the increase of the monomer feeding time yielded a higher gel content. For a given monomer feeding time, the gel content increased with the polymerization temperature. The initial increase of the feeding time from 3 to 12 h led to a substantial increase of gel, but a further increase of the feeding time to 24 h resulted in a modest increase of gel, especially at the highest temperature. These results can be explained considering the mechanisms that lead to the formation of gel polymer in the emulsion polymerization of *n*-BA. Gel is formed by the occurrence of intermolecular chain transfer to polymer followed by bimolecular termination by combination. If this is called a gel-forming event, the gel fraction depends on the ratio between the number of gel-forming events and the propagation

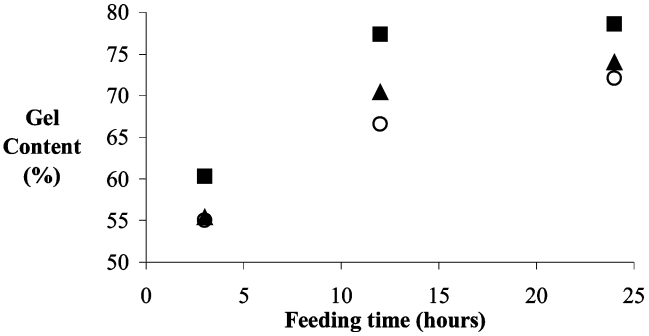

Figure 7. Final gel content of poly(*n*-BA) latexes produced at different feeding times and temperatures. Legend: (○) 75 °C, (▲) 85 °C, (■) 95 °C.

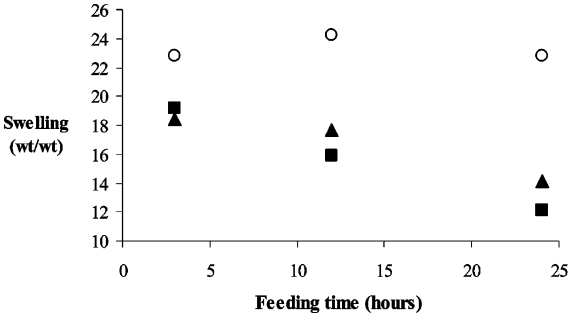

Figure 8. Swelling of poly(*n*-BA) dried latexes produced at different feeding times and temperatures measured in MEK at 25 °C for 24 h. Legend: (○) 75 °C, (▲) 85 °C, (■) 95 °C.

events. The number propagation events was the same in all cases because the same total amount of monomer was polymerized. On the other hand, the number of gel-forming events increased with temperature because of the higher activation energy of the intermolecular chain transfer to polymer as compared with propagation ($E_{a,p} = 17$ kJ/mol, $E_{a,fp} = 29$ kJ/mol).[17,18,23] The number of gel-forming events also increased with the process time because the polymer chains were subjected for a longer time to the action of the radicals. The modest increase in gel observed when the process time increased from 12 to 24 h might be due to the lower radical concentration in the 24 h processes.

Figure 8 summarizes the results obtained in the swelling measurements for the poly(*n*-BA) latexes synthesized at different temperatures and feeding times. Note that the swelling value is inversely proportional to the cross-linking density. Figure 8 shows that the cross-linking density increased with temperature because of the higher number of gel-forming events (i.e., the number of links per macromolecule) and the shorter kinetic length. The same reasons made the cross-linking density to increase with the process time. Admittedly, no explanation can be offered for the low swelling ratio of the latex produced in 3 h at 75 °C. The swelling values achieved at 95 °C and 24 h of monomer addition were close to those produced with 3 h addition and 0.23 mol % of a cross-linker (allyl maleate or diallyl maleate).[26,27]

Figure 9 shows the evolution of the weight-average sol molecular weight of the polymers produced at different monomer feeding times and temperatures. It can be seen that the sol M_w decreased with both increasing monomer feeding time and temperature, the latter effect being smaller at long feeding times. The reason for this behavior is that, because long polymer chains have a higher probability of suffering intermolecular chain transfer to polymer, the gel incorporates preferentially the longer chains, provoking a reduction of the molecular weight of the sol fraction.[2,16]

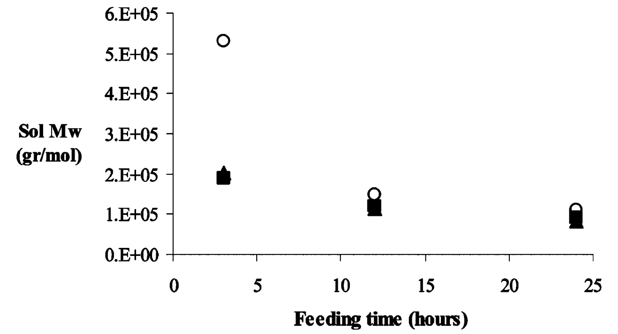

Figure 9. Weight-average sol molecular weight of the final poly(*n*-BA) latexes produced at different feeding times and temperatures. Legend: (○) 75 °C, (▲) 85 °C, (■) 95 °C.

Adhesive Properties of the Poly(*n*-BA) Latexes. Table 4 summarizes the results obtained for the shear resistance and tack tests of some of the poly(*n*-BA) latexes synthesized. It can be seen that the gel content and the shear resistance were strongly correlated. An increase from 55% to 73% of gel content resulted in a 60 times increase of the shear resistance. This effect was likely due to the presence of gel (cross-linking and chain entanglement), which provided a better cohesion in the film. However, the shear resistance dropped dramatically for gel contents above 73%. According to Satas et al.,[28,29] the resistance to shear increases as the molecular weight of the polymer chains increases because this allows a better chain entanglement, which leads to the enhancement of the elasticity of the polymer. However, at very high molecular weights the chain interdiffusion is impeded, and shear resistance drops dramatically. Other sudden decreases of the shear resistance with increasing gel contents have been reported.[5,6,30]

Table 4 also shows that an increase from 55% to 60% of the gel content remarkably decreased the tackiness of the films even though the sol molecular weight decreased.

Conclusions. This work explores the possibility of synthesizing a highly branched poly(*n*-butyl acrylate) by semicontinuous emulsion polymerization. This was achieved by increasing both the monomer feeding time and the polymerization temperature.

Branching levels as high as 6.3% were obtained at high temperature (95 °C) and long feeding times (24 h). The reasons were that the backbiting reaction was favored by increasing temperature because its activation energy was higher than that of the propagation and that long feeding times resulted in very low monomer concentrations in the polymer particles, which promoted intramolecular transfer to polymer. Gel increased with temperature and feeding time. In general, the higher the gel contents, the tighter the network. The shorter kinetic lengths, characteristic of high temperatures and low monomer concentrations, resulted in shorter links between cross-linking points.

Table 4. Shear Resistance and Tack Test Results for Poly(*n*-BA) Latexes Produced at Different Feeding Times and Temperatures

temp (°C)	F time (h)	gel (%)	sol M_w (g/mol)	branches (%)	shear resist (min)	tack (cm)	swelling (w/w)
75	3	55	532 000	2.8	40 ± 10	0.5 ± 0.7	23
85	24	73	81 800	5.8	2500 ± 230	5.0 ± 1.7	16
95	3	60	190 000	3.0	300 ± 40	5.1 ± 2.2	22
95	12	76	120 000	4.0	490 ± 125	7.3 ± 1.2	14
95	24	78	90 200	6.3	401 ± 95	6.9 ± 2.0	12

The polymer microstructure strongly affected adhesion properties. An increase in the gel content from 55% to 73% led to a remarkable improvement of the shear resistance. However, further increase in the gel content resulted in a poorer shear resistance, presumably because chain interdiffusion of the highly cross-linked polymer was difficult. Tackiness was substantially reduced by increasing gel content.

The polymerization kinetics was surprising as the polymerization rate decreased with temperature, this effect being more significant at long feeding times. The reason was the depletion of the initiator at higher temperatures and long feeding times combined with the insensitivity of the apparent propagation rate constant to temperature.

Acknowledgment. The authors thank the financial support provided by the Industrial Liaison Program in polymerization in dispersed media of Polymat (Arkema, Cytec Surface Specialies, Dow, Euroresin, Nuplex Resins, Rohm and Haas and Wacker Chemie). The authors are also grateful to the swelling analysis performed by Dr. Ludivine Bouvier-Fontes.

References and Notes

(1) Plessis, C.; Arzamendi, G.; Leiza, J. R.; Schoonbrood, H. A. S.; Charmot, D.; Asua, J. M. *Macromolecules* **2000**, *33*, 4.

(2) Plessis, C.; Arzamendi, G.; Leiza, J. R.; Schoonbrood, H. A.; Charmot, D.; Asua, J. M. *Macromolecules* **2000**, *33*, 5041.

(3) Scott, G.; Senogles, E. *J. Macromol. Sci.* **1974**, *A8*, 753.

(4) Ahmad, N.; Britton, D.; Heatley, F.; Lovell, P. *Macromol. Symp.* **1999**, *143*, 231.

(5) Plessis, C.; Arzamendi, G.; Leiza, J. R.; Schoonbrood, H. A.; Charmot, D.; Asua, J. M. *Macromolecules* **2001**, *34*, 5147.

(6) Plessis, C.; Arzamendi, G.; Leiza, J. R.; Alberdi, J. M.; Schoonbrood, H. A.; Charmot, D.; Asua, J. M. *J. Polym. Sci., Part A: Polym. Chem.* **2001**, *39*, 1106.

(7) Ahmad, N.; Heatley, F.; Lovell, P. A. *Macromolecules* **1988**, *21*, 2822.

(8) Capek, I. *Polymer* **1994**, *26*, 1154.

(9) Ozdeger, E.; Sudol, E. D.; El-Asser, M. S. *J. Polym. Sci., Part A: Polym. Chem.* **1997**, *35*, 3827.

(10) Sajjadi, S.; Brooks, B. *J. Polym. Sci., Part A: Polym. Chem.* **2000**, *38*, 528; *Chem. Eng. Sci.* **2000**, *55*, 4757; *J. Appl. Polym. Sci.* **2000**, *79*, 582.

(11) Sajjadi, S. *J. Polym. Sci., Part A: Polym. Chem.* **2000**, *38*, 3612.

(12) Luo, Y.; Schork, F.; Deng, Y.; Yan, Z. *Polym. React. Eng.* **2001**, *9*, 183.

(13) Gilbert, B. C.; Lindsay, J. R.; Miline, E.; Withwood, A.; Taylor, P. *J. Chem. Soc, Perkin Trans. 2: Phys. Org. Chem.* **1994**, *2*, 1759.

(14) Yamada, B.; Azukizawa, M.; Yamazoe, H.; Hill, D.; Pomery, P. *Polymer* **2000**, *41*, 5611.

(15) Nikitin, A. N.; Hutchinson, R. A. *Macromolecules* **2005**, *38*, 1581.

(16) Plessis, C.; Arzamendi, G.; Leiza, J. R.; Alberdi, J. M.; Schoonbrood, H. A.; Charmot, D.; Asua, J. M. *Ind. Eng. Chem. Res.* **2001**, *40*, 3883.

(17) Plessis, C.; Arzamendi, G.; Leiza, J. R.; Alberdi, J. M.; Van Herk, A.; Asua, J. M. *Macromol. Rapid Commun.* **2003**, *24*, 173.

(18) Asua, J. M.; Beuermann, S.; Buback, M.; Castignolles, P.; Charleux, B.; Gilbert, R. G.; Hutchinson, R. A.; Leiza, J. R.; Nikitin, A. N.; Vairon, J. P.; Van Herk, A. M. *Macromol. Chem. Phys.* **2004**, *205*, 2151.

(19) Chiefari, J.; Jeffery, J.; Mayadunne, R.; Moad, G.; Rizzardo, E.; Thang, S. *Macromolecules* **1999**, *32*, 7700.

(20) Peck, A.; Hutchinson, R. *Macromolecules* **2004**, *37*, 5944.

(21) *Holding Power of Pressure-Sensitive Tape (Metric)*; Norm PSTC-7M.; American Pressure Sensitive Tape Council, 1986.

(22) *Tack Rolling Ball (Metric);* Norm PSTC-6M.; American Pressure Sensitive Tape Council, 1986.

(23) Arzamendi, G.; Plessis, C.; Leiza, J. R.; Asua, J. M. *Macromol. Theory Simul.* **2003**, *12*, 315.

(24) Behrman, E.; Edwards, J. *Rev. Inorg. Chem.* **1980**, *2*, 179.

(25) Beuermann, S.; Buback, M. *Prog. Polym. Sci.* **2002**, *27*, 191.

(26) Fontes, L.; Pirri, R.; Asua, J. M.; Leiza, J. R. *Macromolecules* **2005**, *38*, 1164.

(27) Fontes, L.; Pirri, R.; Arzamendi, G.; Asua, J. M.; Leiza, J. R. *J. Polym. Sci., Part A: Polym. Chem.* **2005**, *43*, 4684.

(28) Satas, D. In *Handbook of Pressure Sensitive Adhesive Technology*; Van Nostrand Reinhold: New York, 1989.

(29) Satas, D. *Adhes. Age* **1972**, *15*, 19.

(30) Alarcia, F.; de la Cal, J. C.; Asua, J. M. *Macromol. Mater. Eng.* **2006**, *291*, 428.

MA060603G